

Supporting Information

Facile Synthesis of Wide Bandgap ZrS₂ Colloidal Quantum Dots for Solution Processed Solar-Blind UV Photodetectors

Zan Wang^{a, b, c, d}, Yunjiao Gu^{b, c, d}, Fenghua Liu^{b, c, d}, Weiping Wu*^{b, c, d}

^a. Institute of Photonics, Department of Optics and Optical Engineering, University of Science and Technology of China, Hefei, Anhui, 230026, China

^b. Laboratory of Thin Film Optics, Shanghai Institute of Optics and Fine Mechanics, Chinese Academy of Sciences, Shanghai, 201800, China

^c. State Key Laboratory of High Field Laser Physics, Chinese Academy of Sciences, Shanghai, 201800, China

^d. University of Chinese Academy of Sciences, Beijing, 100049, China

E-mail: wuwp@siom.ac.cn

Experimental Section

Chemicals: zirconium chloride (ZrCl_4 , >99.9%, Aladdin, China), 1-dodecanethiol (DT, 98%, Acros, Belgium), 1,2-ethanedithiol (EDT, 98.0%, Alfa Aesar, UK), oleylamine (OAm, 80%, Acros, Belgium). All these reagents were of analytical grade and used without further purification.

Synthesis of ZrS_2 QDs: A one-pot method to synthesize the ZrS_2 QDs is as follows. a mixture of ZrCl_4 (0.14 g, 0.6 mmol), DT (1.7 mL, 10 mmol), and OAm (8 mL) was loaded in a 100 mL three-neck flask. The mixture was heated to 100 °C and maintained for 30 min to remove oxygen from the slurry with vigorous magnetic stirring under a vacuum. Afterward, the reaction temperature was raised to 225 °C and retained at this temperature for 1.5 hours to allow the growth of ZrS_2 QDs under the N_2 atmosphere. The products were mixed with excess butanol and precipitated through centrifugation at 12000 rpm for 20 minutes. The ZrS_2 QDs are washed with hexane (4.0 mL) and methanol (8.0 mL). Finally, the ZrS_2 QDs were dispersed in cyclohexane solvent and stored in an atmospheric environment for further use.

The 1-dodecanethiol was chosen as the sulfur precursor to produce a slow and continuous influx of H_2S in situ, which reacts with ZrCl_4 in oleylamine and the formation of ZrS_2 QDs after maintaining this temperature for 1.5 hours.

Fabrication of the photodetector devices: The device fabrication process begins with cleaning the glass substrates by using acetone and isopropanol and UV-ozone treatment for 15 min to remove organic contaminations on the surface of the glass. The ZrS_2 QDs solution was deposited on the substrate by spin-coating method (1500 rpm, 30 s). Then, 300 μL ligand solution (5 mM EDT in acetonitrile) was dispensed onto the QDs film, kept for 30 s, and spun to dry. The substrate was then submerged in acetonitrile three times to remove residual unbound ligands. The processes of spin-coating and ligand exchange were repeated 6 times. Finally, 5 nm/100 nm thick Ti/Au metal electrodes were deposited through an interdigitated shadow mask through a thermal evaporator coating to achieve Au/ ZrS_2 /Au PD structure.

Characterizations: The morphologies of the ZrS_2 QDs and the high-angle annular dark-

field scanning transmission electron microscopy (HAADF-STEM) and energy-dispersive X-ray spectroscopy (EDS) elemental mappings were examined using an FEI Talos F200X TEM at 200 kV. Powder X-ray diffraction (XRD) patterns were measured by a PANalytical Empyrean Powder X-ray diffractometer with Cu-K α radiation ($\lambda=1.54056$ Å). The X-ray photoelectron spectroscopy (XPS) was conducted on a Thermo Scientific K-Alpha instrument using Al K α (1486.6 eV) X-ray source.

The Raman spectrum was obtained at an ambient temperature on a HORIBA JOBIN YVON Labram Aramis Raman Spectrometer with an excitation wavelength of 532 nm. The optical absorption spectra were tested using a Shimadzu UV2600 ultraviolet-visible (UV-Vis-NIR) spectrometer. The photoluminescence (PL) spectra were recorded on a Shimadzu PF-5301PC fluorescence spectroscopy-fluorometer. The photoelectric properties of the devices were investigated and measured using a Keithley 4200-SCS semiconductor characterization system and a Signatone S-1160 probe station.

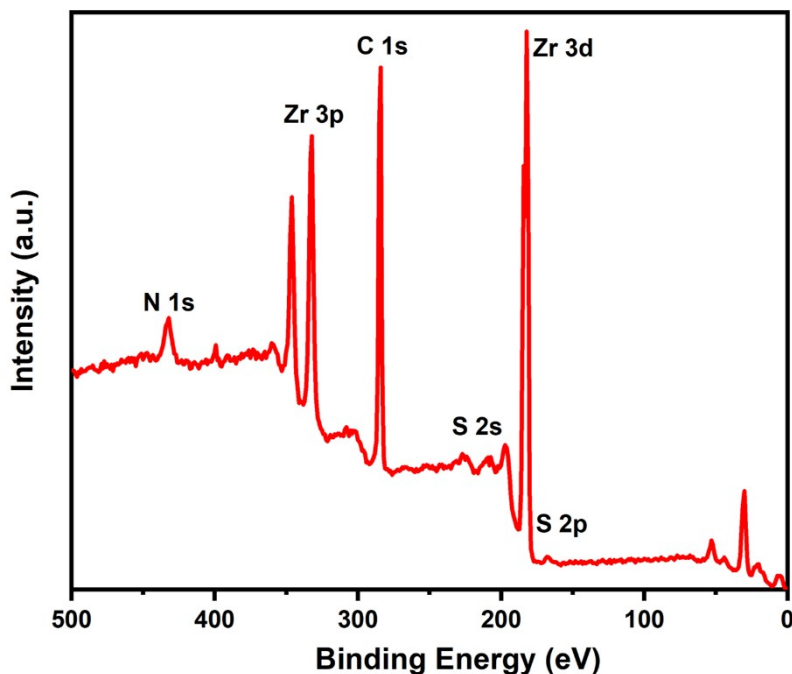


Figure S1. The survey XPS spectra of the ZrS₂ QDs.

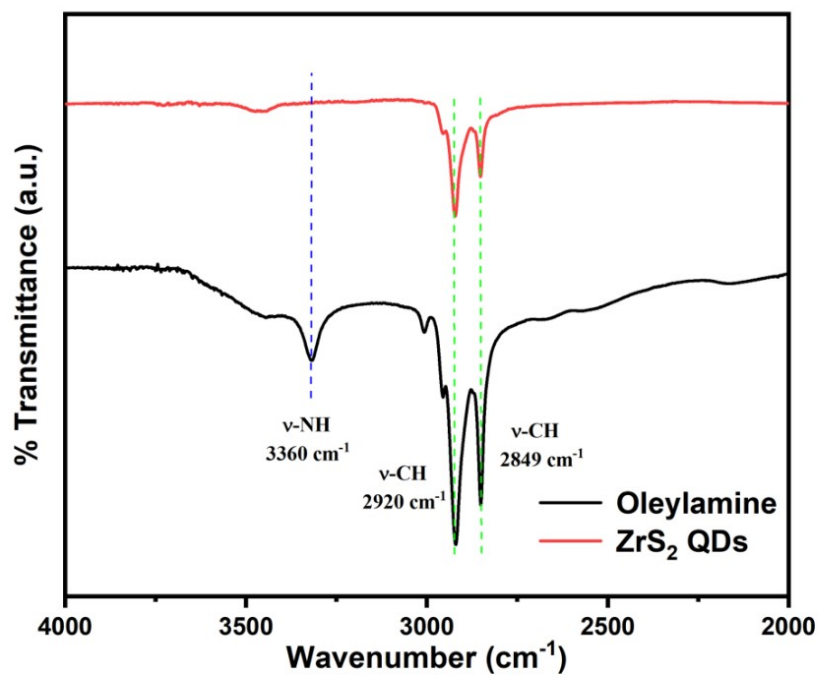


Figure S2. The FTIR spectra of the raw oleylamine and ZrS₂ QDs.

FTIR spectra of ZrS₂ QDs show the symmetric and asymmetric CH₂ stretching is located at about 2849 and 2920 cm⁻¹ respectively¹, which could be observed in the spectrum of raw oleylamine and ZrS₂ QDs (Figure S2). Further, the peak 3360 cm⁻¹ is due to N-H stretching vibration and attributed to amino groups, which is a feature of raw oleylamine.² Thus, the disappearance of this peak on the ZrS₂ QDs indicated that there is a strong binding that exists between oleylamine and ZrS₂ QDs, which is also evidence that oleylamine acts as a ligand on the surface of the ZrS₂ QDs.¹⁹

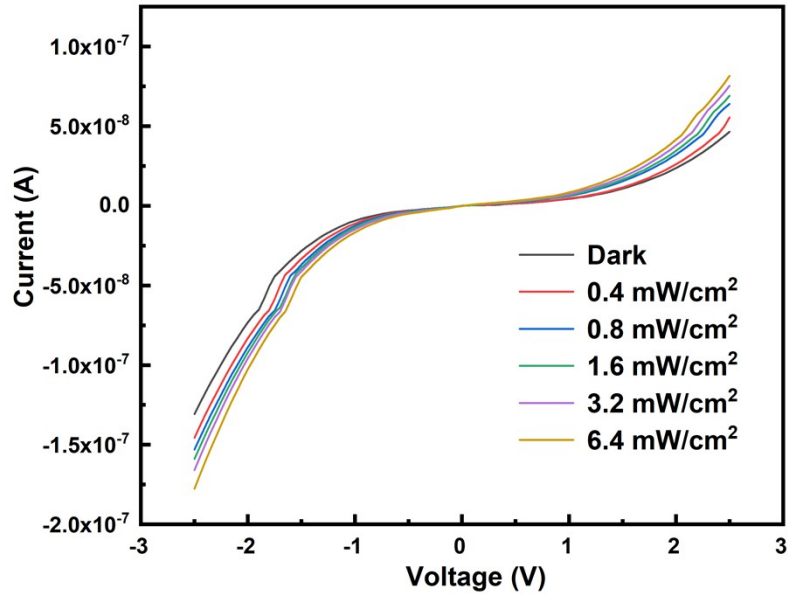


Figure S3. The I-V characteristics of the fabricated ZrS₂ QDs-based PD in dark and under 365 nm UV light with different power densities.

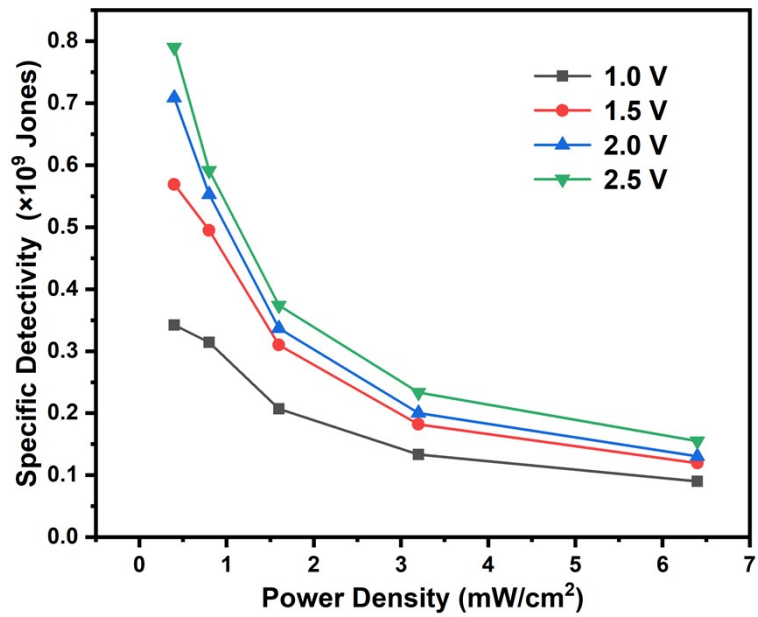


Figure S4. The specific detectivity of ZrS₂ QDs-based PD was described as the dependence of power density under 365 nm UV illumination at various applied bias voltages.

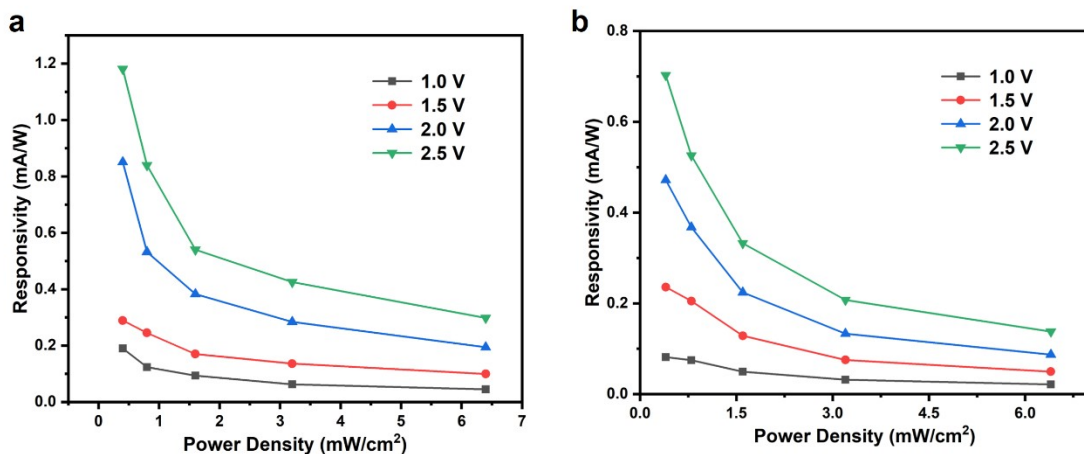


Figure S5. The responsivity of ZrS_2 QDs-based solar-blind PD was described as the dependence of power density at various applied bias voltages (a) under 254 nm UV illumination and (b) under 365 nm UV illumination.

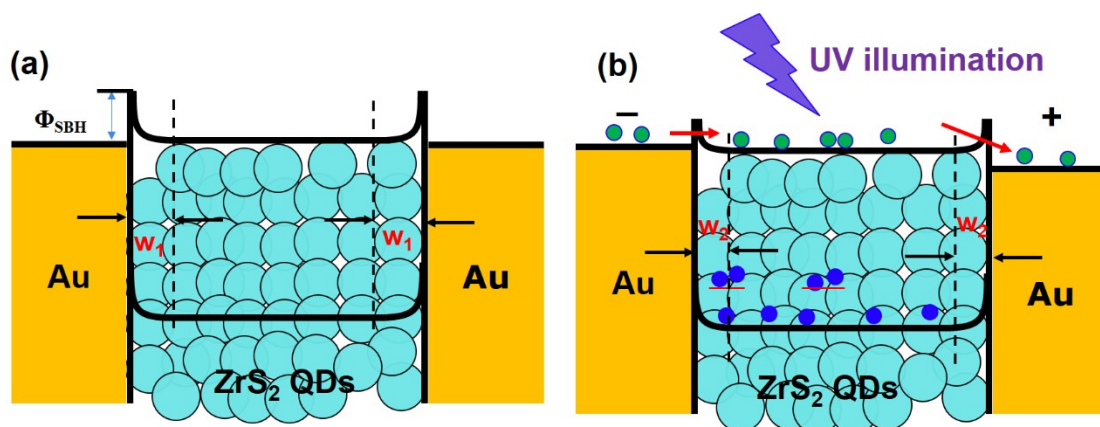


Figure S6. The schematic of energy band diagrams of Au/ ZrS_2 QDs/Au PD on glass substrate with proper electron-hole transport mechanism (a) under dark and without external bias, (b) under illumination and with external bias.

The schematic of energy band diagrams of Au/ZrS₂ QDs/Au PD on a glass substrate with proper electron-hole transport mechanism is shown in Figure 6. Figure 6a shows the band diagram of the PD in the dark and without external bias. The Au-metal and ZrS₂ QDs formed Schottky contact, therefore, there is a small barrier height (Φ_{SBH}) at the Au-ZrS₂ QDs junction. Under UV illumination and with external bias, the trap states of ZrS₂ QDs, structural defects and vacancies, serve as trapping centers for photogenerated holes (Figure S6b). This results in a reduction in the depletion region width (w_2) and Φ_{SBH} , which offers favoring conditions for electrons tunneling into the semiconductor to maintain charge neutrality, causing increased photocurrent.

Device parameter calculations: The representative parameters (responsivity R , special detectivity D^*) of the UV and solar-blind photodetector devices were determined as follows,

$$R = \frac{I_{ph} - I_d}{P} \quad (S1)$$

$$D^* = \frac{A^{1/2} gR}{(2qg_d)^{1/2}} \quad (S2)$$

where I_{ph} is the photocurrent, I_d is the dark current, P is the radiated power (product of area and incident light density), A is the active area of the photodetector, q is the electron charge.

References

1. Z. Wang, F. H. Liu, Y. J. Gu, Y. G. Hu and W. P. Wu, *J. Mater. Chem. C*, 2022, **10**, 1097-1104.
2. W. X. Yin, X. Bai, P. Chen, X. Y. Zhang, L. Su, C. Y. Ji, H. M. Gao, H. W. Song and W. W. Yu, *ACS Appl. Mater. Interfaces*, 2018, **10**, 43824-43830.